Determination of Precipitation Profiles from Airborne Passive Microwave Radiometric Measurements

CHRISTIAN KUMMEROW*

Laboratory for Atmospheres, Goddard Space Flight Center, Greenbelt, Maryland

IDA M. HAKKARINEN AND HAROLD F. PIERCE

General Sciences Corporation, Laurel, Maryland

JAMES A. WEINMAN

Space Science and Engineering Center, University of Wisconsin, Madison, Wisconsin

(Manuscript received 30 April 1990, in final form 30 August 1990)

ABSTRACT

This study presents the first quantitative retrievals of vertical profiles of precipitation derived from multispectral passive microwave radiometry. Measurements of microwave brightness temperature (Tb) obtained by a NASA high-altitude research aircraft are related to profiles of rainfall rate through a multichannel piecewise-linear statistical regression procedure. Statistics for Tb are obtained from a set of cloud radiative models representing a wide variety of convective, stratiform, and anvil structures. The retrieval scheme itself determines which cloud model best fits the observed meteorological conditions. Retrieved rainfall rate profiles are converted to equivalent radar reflectivity for comparison with observed reflectivities from a ground-based research radar. Results for two case studies, a stratiform rain situation and an intense convective thunderstorm, show that the radiometrically derived profiles capture the major features of the observed vertical structure of hydrometeor density.

1. Introduction

Concern has been mounting regarding change in the global climate. This interest has been triggered by the increased concentration of carbon dioxide and methane in the lower atmosphere and the decreased concentration of ozone in the stratosphere. These changes ultimately can alter radiative heating profiles in the atmosphere. On a more immediate time scale is the shorter-term climatic change brought about by variations in sea surface temperatures and rainfall. Within precipitating regions, latent heating distributions are altered drastically by condensation and evaporation processes. Sustained periods of anomalous latent heating have the potential of modifying not only the immediate environment, but also the global circulation.

The vertical distribution of latent heating is especially significant because it affects atmospheric stability. Lau and Peng (1987) showed that the distribution of latent heat in tropical convective systems had an impact upon the propagation speed of Kelvin waves, which are intimately related to 30–60 day oscillations in the tropics. Modeling work by Trenberth et al. (1988) indicated that the vertical profiles of latent heating in the tropical Pacific region were correlated with the recent North American drought.

The global distributions of rainfall near the surface have been derived from satellite observations made at visible, infrared, and microwave frequencies (Theon and Fugono 1988). This information is useful, but it cannot address the problem of latent heating distributions as these are known to vary greatly for different types of clouds. Convective clouds, for instance, introduce heat of condensation into the entire atmosphere up to heights of ~10 km, while stratiform clouds may heat the atmosphere between 5 and 10 km and cool it below 4 km by melting and possibly by evaporation (Houze 1982). Quantitative vertical profiles of precipitation have not been obtained heretofore from remotely sensed imagery.

Weather radar data usually are displayed in two formats: 1) the plan-position indicator (PPI) mode and 2) the range–height indicator (RHI) mode. The PPI displays the range and azimuth of precipitation echoes in polar coordinates at a fixed elevation angle; the RHI displays the slant range and elevation angle of the precipitation echoes along a given azimuth from the radar.

* Universities Space Research Association resident associate.

Corresponding author address: Dr. Christian Kummerow, Severe Storms Branch, Code 612, NASA/Goddard Space Flight Center, Greenbelt, MD 20771.

Both displays are intensity-modulated, producing an echo whose brightness corresponds to the target signal strength. Weather radar observations of this type are mainly obtained from land regions in developed countries. Global observations of the vertical distribution of precipitation, however, will only be possible from spaceborne sensors. X-band (3-cm wavelength) radars have been flown on the Soviet Cosmos series of spacecraft (Pichugin and Spiridonov 1987). Although imagery from these radars have revealed the existence of rain cells, no spaceborne radar measurements of the vertical structure of precipitation have been published. A spaceborne radar that will yield vertical precipitation profiles is planned for the Tropical Rainfall Measuring Mission (TRMM) (Simpson et al. 1988), but it is not scheduled for launch until 1996.

This study will present vertical cross sections of precipitation derived from brightness temperatures, Tb, obtained from multichannel passive microwave radiometry. Passive radiometry, unlike radar, measures the radiation emanating from the earth's surface and precipitating hydrometeors in accord with the Planck radiation law. Ultimately, it is desirable to make such measurements from spacecraft; however, airborne microwave radiometers have better spatial resolution than similar radiometers that are now on spacecraft, thus allowing better comparisons with ground-based radar measurements.

Measurements at 18 and 37 GHz made from the Microwave Precipitation Radiometer (MPR) and at 92 GHz from the Advanced Microwave Moisture Sounder (AMMS) aboard the NASA ER-2 high-altitude aircraft flying above the cloud tops are used in this study. The characteristics of the radiometers and the aircraft are summarized in Table 1. These data were obtained during the Cooperative Huntsville Meteorological Experiment (COHMEX) conducted during the summer of 1986 (Dodge et al. 1986). The retrieved profiles are compared with coincident RHI imagery provided by the NASA SPANDAR radar located at Wallops Island, Virginia. Some characteristics of this radar are also shown in Table 1.

2. Method

The observed microwave brightness temperatures, Tb, originate partly at the earth's surface and partly from atmospheric constituents. The contribution from the earth's surface primarily depends upon the nature of the surface (i.e., water or land) and on the temperature of that surface. Atmospheric constituents such as oxygen, water vapor, and cloud water act to absorb and emit upwelling radiation. Large, precipitation-size drops further act to scatter upwelling radiation. In precipitation, the contribution from atmospheric constituents primarily depends upon the concentrations of cloud water, raindrops, and ice particles, as well as the vertical distribution of these quantities. To a lesser degree, the brightness temperatures further depend upon the hydrometeor drop-size distributions, the temperature and water vapor profiles within the cloud, and the characteristics of the underlying surface. The relative importance of these parameters is a function of both the nature of the precipitating cloud and the microwave frequency being used for observation.

The vertical distribution of hydrometeors is crucial in determining the microwave brightness temperatures. It cannot, however, be easily characterized in terms of a single variable, as is done with the surface rain rate or the low-level cloud liquid water. Thus, we employ a set of cloud radiative models. Each model consists of five vertical layers and completely specifies a distinct cloud vertical structure in terms of "near surface" parameters (rain rate and cloud liquid water). Previous experience, alternate data sources, cloud microphysical models, or climatological information can be used to

TABLE 1. Characteristics of the ER-2 aircraft, microwave radiometers, and the SPANDAR radar.

Aircraft:					
Altitude					20 km
Nominal cruising speed					205 m s^{-1}
Microwave radiometers					
Frequency (GHz)	Instrument	Accuracy (K)	Polarization	Horizontal Resolution (km)	View angle (deg)
18	MPR	±1.0	H, V	3.3	45
37	MPR	±1.0	H, V	1.7	45
92	AMMS	±0.5	—	0.7	0
Radar					
Wavelength					10.56 cm
Range resolution					200 m
Angular resolution					0.4°

make these assumptions as realistic as possible. Twenty-five distinct cloud models covering a wide variety of convective, stratiform, and anvil clouds were constructed. Samples of the cloud models are shown in Fig. 1. Ten of these models were "convective" (see Figs. 1a,b). A convective cloud model, in the present context, is defined as a cloud containing a significant amount of liquid water above the freezing level, the water having been carried aloft by strong updrafts within the cloud. Such models have also been described by Smith and Mugnai (1989) as "cold rain with a mixed layer," indicating the presence of significant quantities of both liquid and frozen drops above the freezing level. Ten cloud models are defined as "stratiform" (see Fig. 1c), indicating the absence of liquid water above the freezing level. Such clouds are often associated with horizontally homogeneous precipitation related to frontal passages or with the decaying portions of thunderstorms. Five cloud models are defined as "anvil clouds" (see Fig. 1d). These models are characterized by ice aloft, but no significant precipitation at the surface. Such clouds are often observed in blowoff regions of strong convection. Cirrus clouds are a typical example of this type of structure. The structures described here are quite general and are not designed for specific circumstances. The retrieval scheme itself determines which of these 25 cloud models best fits the observed meteorological conditions. The only information supplied a priori in this study was the nature of the underlying surface (land or water). This information was obtained using the aircraft navigation record.

Retrievals are performed separately for each cloud radiative model. This study uses a multifrequency piecewise-linear regression technique (Chang and Milman 1982; Kummerow 1987) to interpret observed Tb's in terms of profiles of the rainfall rates. The parameterized quantities in each candidate cloud structure (surface rainfall and cloud liquid water), along with the surface temperature, and wind speed over water or emissivity over land, are varied randomly to generate a large set of possible clouds. Multiple linear regression methods are then applied to the brightness temperatures derived through the radiative transfer scheme to obtain regression coefficients relating the geophysical parameters of interest (i.e., surface rainfall rate) to a linear combination of the observed brightness temperatures. This can be expressed as

$$R = a_0 + \sum_{i=1}^{N} a_i Tb_i \qquad (1)$$

where R is the surface rainfall rate (in mm h^{-1}), N is the total number of available channels, a_0 and a_i are the regression coefficients, and Tb_i is the brightness temperatures for each channel i, respectively.

Unfortunately, the rainfall rate is a highly nonlinear function of the brightness temperature. A linear regression technique thus offers limited promise for retrieving rainfall over the large range of possible values. This problem is ameliorated by performing separate regression analyses over six rainfall rate intervals: 0–3, 3–6, 6–10, 10–20, 20–40, and 40–100 mm h^{-1}. Within these intervals, the brightness temperatures at each microwave frequency are approximately linear functions of rainfall rate. Details of the above procedure, the radiative transfer scheme, and the method used to select the appropriate rainfall interval are described in Kummerow et al. (1989).

By requiring consistency between observed Tb's and those calculated from the cloud radiative models at all frequencies for a given set of retrieved parameters, it is possible to select the cloud radiative model that best represents the specific rain cloud being observed. This is accomplished using the process shown in Fig. 2. If the cloud radiative model accurately represents the underlying rain scene, then it will generate multifrequency sets of brightness temperatures that are very similar in nature to the observed Tb's. This, in turn, produces retrieved quantities whose corresponding brightness temperatures closely resemble the observations. The converse of this is true only if a given set of brightness temperatures corresponds to a unique set of geophysical parameters. Although no proof of uniqueness is given here, simulations show that acceptable results can be obtained as long as the total number of independent radiometric channels exceeds the number of free and parameterized variables needed to adequately describe a given rain profile.

The hydrometeors are assumed to follow a Marshall–Palmer drop-size distribution (Marshall and Palmer 1948). The hydrometeors are further assumed to be oblate spheroids whose semimajor and semiminor axes depend upon r, the equivalent sphere radius prescribed by the Marshall–Palmer drop-size distribution (see Kummerow and Weinman 1988). The radiative transfer calculations are performed using an Eddington approximation to account for absorption, emission, and scattering. The surface can be either Lambertian (for land cases) or bireflecting (for ocean cases).

Although this procedure retrieves rainfall rates (R) (in mm h^{-1}), the results have been converted to equivalent radar reflectivity (Z), (expressed in dBZ) to allow direct comparison with the observed radar reflectivity. Because the retrieval assumes that the hydrometeors follow a Marshall–Palmer drop-size distribution, the Z–R relation applicable to this distribution must also be used to convert the retrieved rainfall rate to an equivalent reflectivity. For liquid drops, $Z = 200R^{1.6}$ is used, while $Z = 1000R^{1.6}$ is used for frozen drops according to Smith (1984).

3. Case studies

The COHMEX field program provided a unique dataset consisting of high spatial resolution radiometric

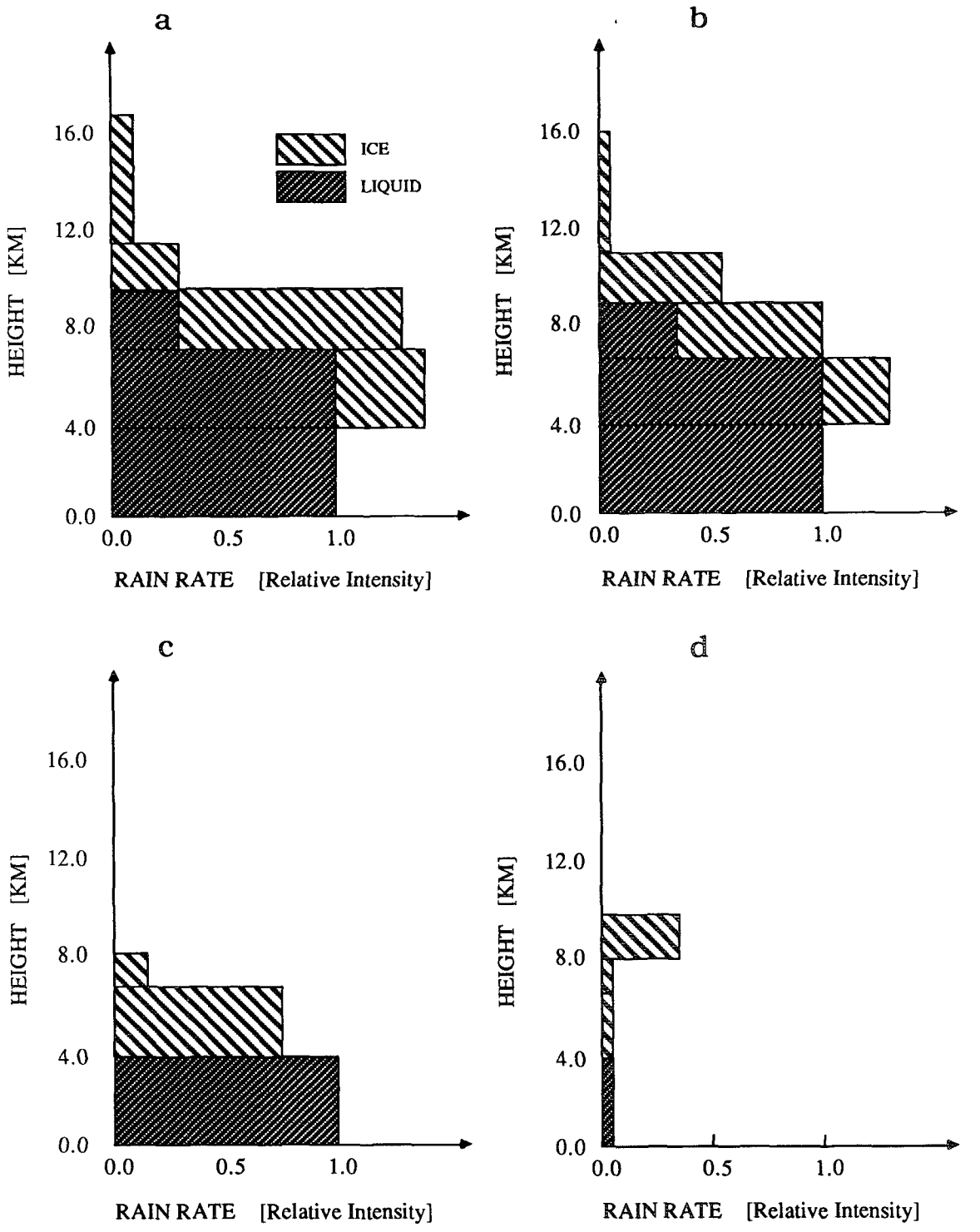

FIG. 1. Schematic diagram of the vertical distribution of cloud constituents in four examples of the five-layer cloud model, (a, b) convective models, (c) stratiform rain model, (d) cirrus anvil model.

measurements from a NASA high-altitude ER-2 aircraft with coincident ground truth measurements provided by well-calibrated surface radars. The ER-2 aircraft flew two special missions during COHMEX within range of NASA's SPANDAR radar at Wallops Island, Virginia. The first case to be discussed is from 1 July 1986, when the aircraft overflew light stratiform rain over the ocean. The second case presented is from

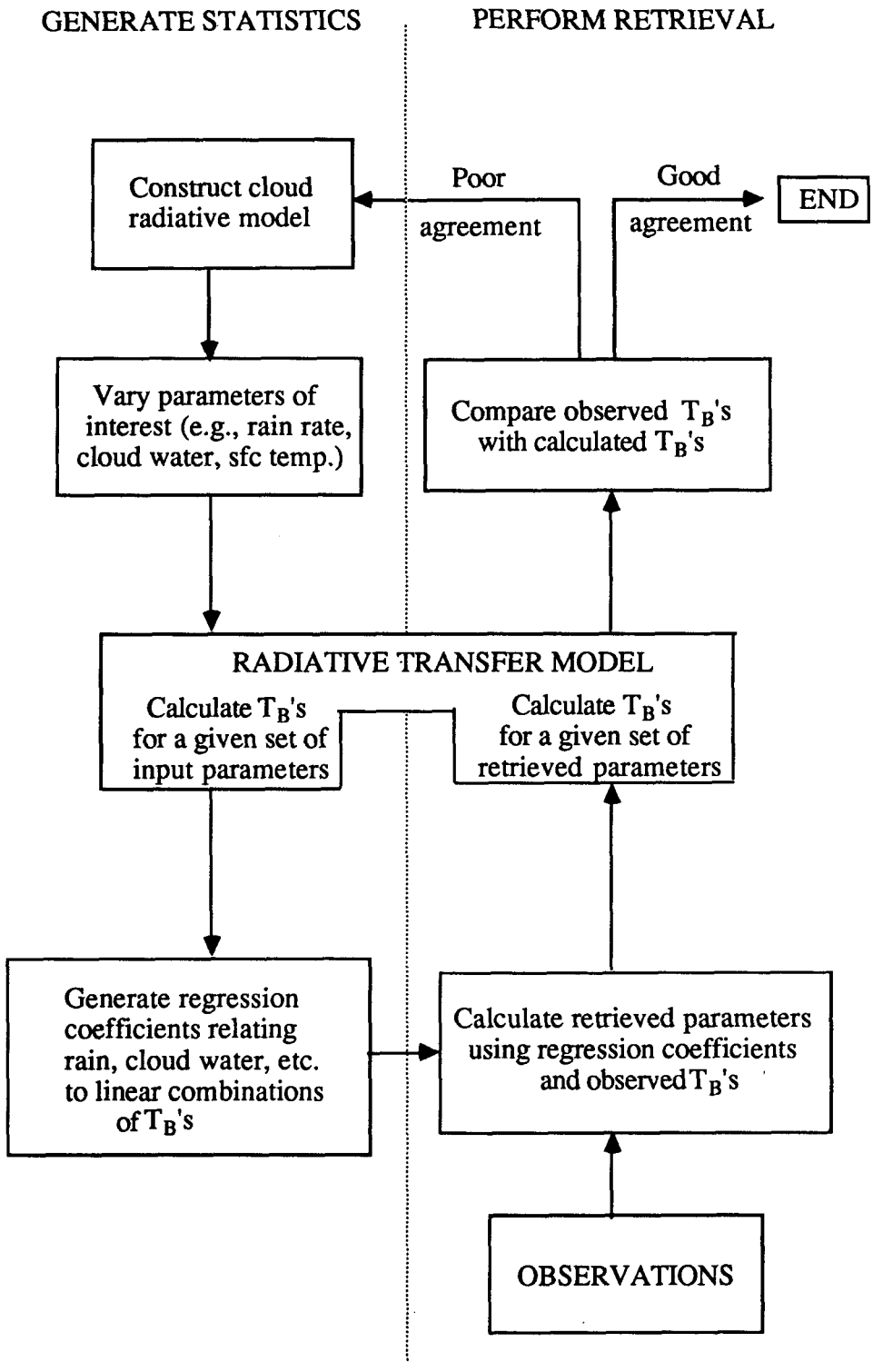

FIG. 2. Flow chart showing the procedure used to select the cloud radiative model parameters that best fit the ensemble of measured brightness temperatures.

29 June 1986, when the aircraft made two passes over deep convection with intense rainfall along the North Carolina–Virginia border. An independent data analysis on the second case has been conducted by Adler et al. (1990).

Retrievals were performed using 5-km horizontal resolution in order to simulate data that might be obtained from planned satellite missions such as TRMM or the Earth Observing System (EOS). Although data were collected with slightly higher spatial resolution (see Table 1), the brightness temperatures were averaged to assure uniform spatial resolution in all five channels and to simulate future satellite missions. Because the AMMS scans across-track along nadir while the 18- and 37-GHz channels on the MPR look forward at a fixed view of 45°, the two sensors view slightly different scenes at any given time. To account for this difference in the two measurements, maximum and minimum brightness temperatures observed for features found in both the 37- and the 92-GHz channels were sampled. A regression analysis was performed relating the 37-GHz channel Tb's with the time offset from the 92-GHz Tb's. The times of the MPR observations were then adjusted to match more closely in time with the AMMS nadir observations, thus minimizing the differences in the two datasets due to differences in sensor viewing geometry.

a. Stratiform rain case—1 July 1986

On 1 July, the NASA aircraft overflew light stratiform precipitation off the coast of the Delmarva peninsula near Wallops Island, Virginia. Since the flight line is over the radiometrically cold ocean, rainfall is characterized by warmer Tb values associated with the thermal emission of raindrops. The retrieval, in this case, must be able to discriminate between the precipitation and the cloud water, both of which tend to increase microwave brightness temperatures. During the aircraft overpass, the radar was operating in RHI mode in order to collect data along the vertical plane defined by the aircraft track as the plane flew along the 120° radial.

Figure 3a shows the corresponding observed radar reflectivities along the two flight lines of the aircraft. The narrow strip of artificially high reflectivities at ~4 km is a result of the "bright band" effect, caused by the increased reflectivity of melting ice particles falling through the freezing level. The bright band is frequently found in light precipitation situations (Ramana Murty et al. 1965).

Figure 3b shows the reflectivities derived from the five-layer rainfall structure obtained through the retrieval procedure described previously. A nominal aircraft altitude of 20 km was assumed in order to determine the position of the surface rainfall relative to the 45° forward-viewing geometry of the 18- and 37-GHz radiometer. This adjustment of the radiometer data allows direct comparison between reflectivities obtained from the radar and the airborne microwave radiometric measurements.

The retrieved reflectivity profiles along the flight line compare quite well with the observed radar reflectivities. It is clear from the vertical structure of the retrieved profile that only stratiform cloud models were selected by the retrieval for this situation. The bright band does not appear in the retrieved vertical reflectivity profiles. This is a natural consequence of it not having been included in the cloud models. Current understanding of radiative transfer through melting layers is still very crude. Moreover, a close examination of the brightness temperatures in this case revealed that the bright band is not very significant in determining the radiation emitted at the frequencies under consideration. Much more important is the presence of variable quantities of cloud water. More investigations, such as those recently undertaken by Vivenkanandan et al. (1989), are needed to resolve the bright band problem.

Quantitative comparisons between observed radar reflectivities and those inferred by the retrieval algorithm for the two flight lines are shown in Fig. 4. Shaded contours represent regions in which there are more than 150 and 500 points with the same observed and retrieved reflectivities. The line of perfect agreement is shown for reference. The regression lines of best fit through the points are given by

$$\mathrm{dBZ(retrieved)} = 6.0 + 0.7\ \mathrm{dBZ(radar)}, \quad \text{flight line 1} \qquad (2)$$

$$\mathrm{dBZ(retrieved)} = 6.2 + 0.7\ \mathrm{dBZ(radar)}, \quad \text{flight line 2.} \qquad (3)$$

The correlation coefficients are 0.68 and 0.65, respectively.

The line of best fit does not pass through the origin because the retrieval scheme considers only five vertical layers. Thus, it tends to produce results with a sharp cutoff at the cloud top, while the observed radar reflectivities taper off much more gradually. Coupled with this is the exponential relationship between rainrate and reflectivity. A 1 mm h^{-1} rain rate represents a reflectivity value of ~25 dBZ. Points lying on either of the axes in Fig. 4 are therefore not of great concern, since they are below this threshold. The high reflectivity values, representing most of the rain, lie fairly well along the line of perfect agreement.

b. Intense convective rain case—29 June 1986

On 29 June, the ER-2 aircraft made two passes over intense convection along the North Carolina–Virginia border. The aircraft flew along a line of cells that extended from the northeast (125 km from the radar) to the southwest (225 km from the radar). Maximum radar reflectivities > 50 dBZ were observed along this

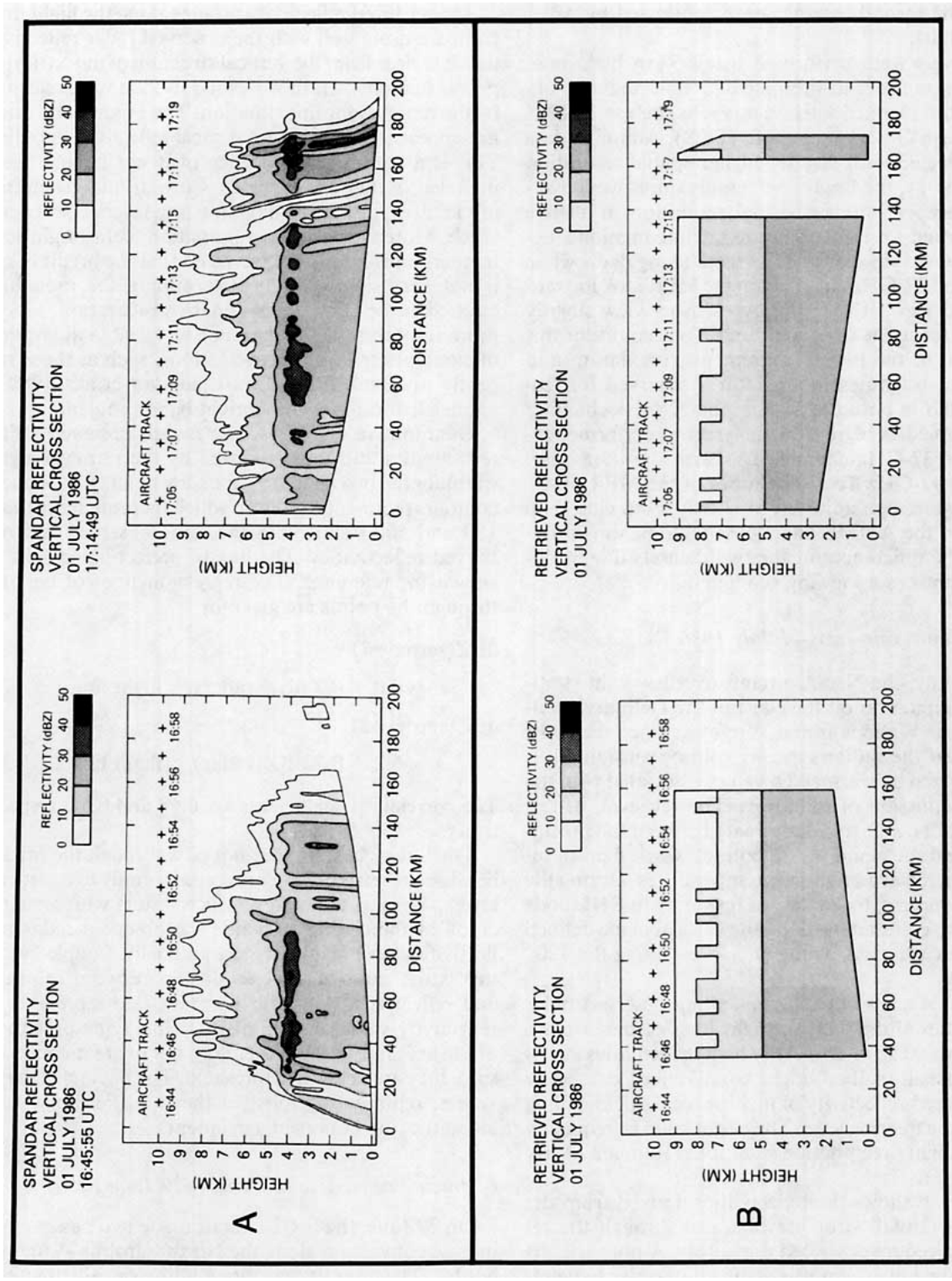

FIG. 3. Observed and retrieved reflectivities (dBZ) corresponding to the light precipitation over water off the coast of Virginia on 1 July 1986. (a) Radar-measured reflectivities. (b) Reflectivities deduced from the retrieval scheme applied to the aircraft measured brightness temperatures.

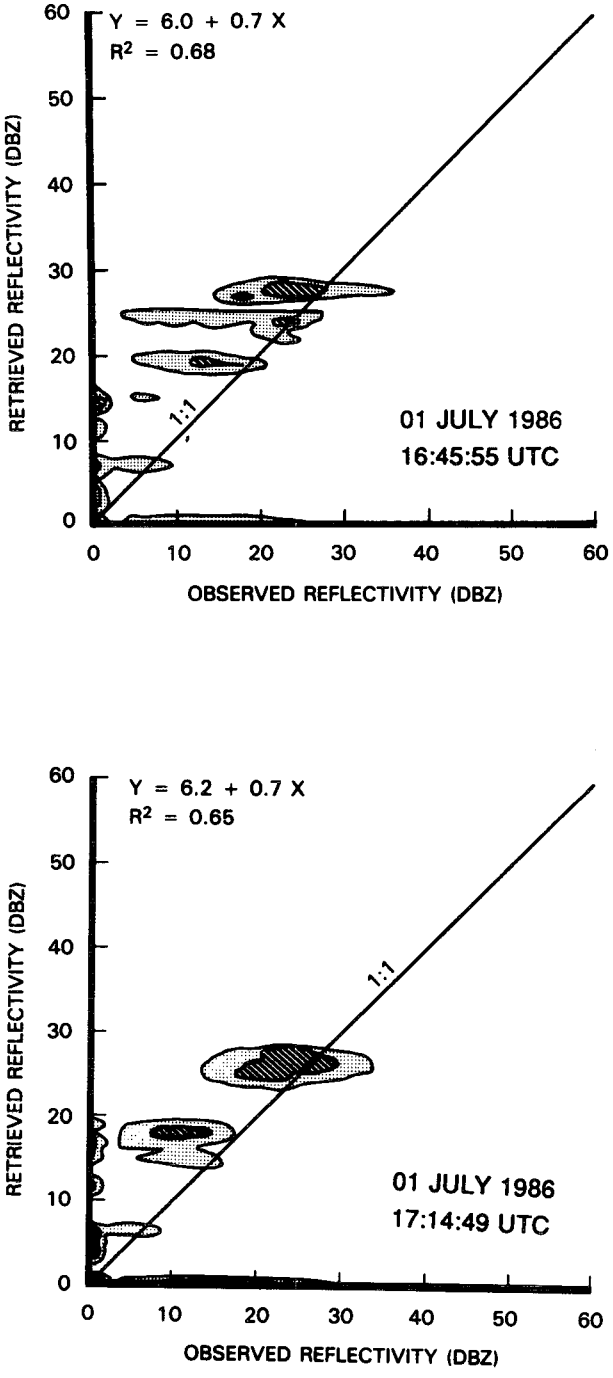

FIG. 4. Scatter plots showing correlation between observed radar reflectivities and retrieved reflectivities for the 1 July 1986 case study. Shaded contours represent regions containing more than 150 and 500 points with the same observed and retrieved reflectivities.

line. Such reflectivities correspond to rainfall rates of greater than 80 mm h^{-1}.

This case is representative of intense convective activity with very large rainfall rates over a land background. Much of the microwave signature in this case is a result of the scattering of radiation away from the direction of the radiometer, which produces brightness temperatures over the storm that are much colder than the surrounding land. At 92 GHz, the intense thunderstorm cores produced brightness temperatures as low as 70 K. Even at 18 GHz, a minimum of 195 K was reached. These low brightness temperatures are caused by very large concentrations of ice particles in the middle and upper portions of the storm cores.

Figure 5a shows reflectivities along flight lines 1 and 2 derived from the radar vertical cross section along the flight track. Since the flight lines in this case were not along a radial, these cross sections were generated from volume scan data taken by the SPANDAR radar. Regions of very intense echoes are evident along the flight path. For example, a cell at 62 km along the cross section of flight line 1 has reflectivities > 40 dBZ extending to ~13 km.

In this example, the retrieval procedure selected convective, stratiform, and anvil structures. Reflectivities derived from the retrieved rainfall structure are shown in Fig. 5b. Anvil structure retrievals are not visible in the figures, as they were retrieved outside the range of the radar in the downwind direction of the storm. Clearly evident, however, are the stratiform and convective retrievals. The stratiform cloud models are characterized by vertical structures that do not exceed ~8 km, while the convective models are, in general, allowed to reach higher altitudes. The retrievals properly identify the regions of strong updrafts (characterized by the high reflectivities of liquid water reaching high into the cloud) as well as the regions where the storm is in a decaying phase.

The quantitative comparisons between observed and retrieved radar reflectivity are shown in Fig. 6. Shaded contours represent regions in which there are more than 200 and 500 points with the same observed and retrieved reflectivities. The regression lines of best fit through the points are given by:

$$\mathrm{dBZ(retrieved)} = -4.3 + 0.9\ \mathrm{dBZ(radar)}, \quad \text{flight line 1} \quad (4)$$

$$\mathrm{dBZ(retrieved)} = 5.5 + 0.8\ \mathrm{dBZ(radar)}, \quad \text{flight line 2.} \quad (5)$$

The correlation coefficients are 0.62 and 0.65, respectively.

The high reflectivity values, representing most of the rain, can again be seen to lie rather well along the line of perfect agreement, although the retrievals seems to consistently overestimate the reflectivities somewhat for flight line 1. The origin of the overestimate is not known explicitly but there are a number of factors that could contribute to this problem. The observed reflectivities may be an underestimate of the true reflectivity as a result of the spreading of the radar beam for rain cells very far away from the radar (~200 km in this

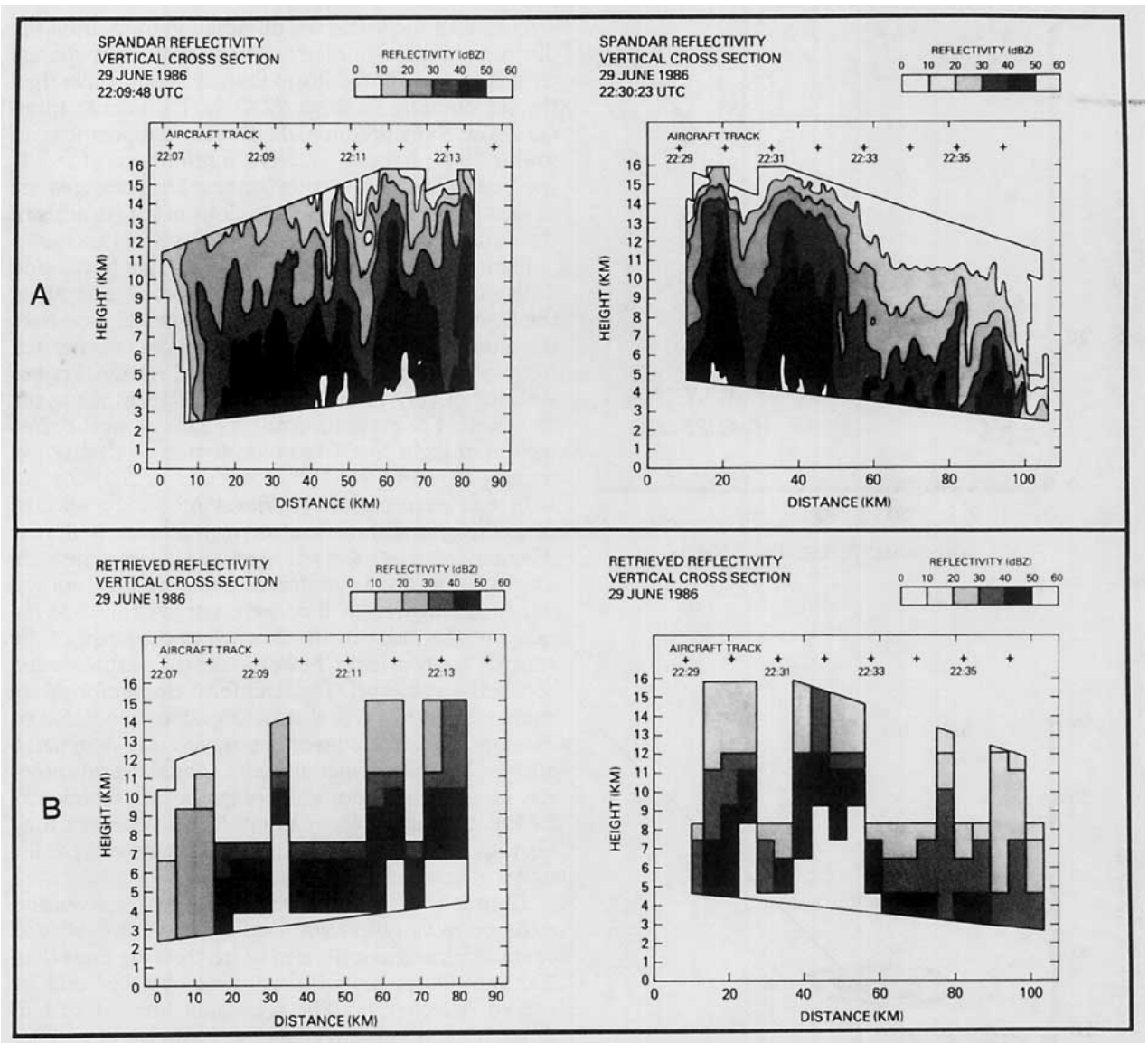

FIG. 5. Observed and retrieved reflectivities (dBZ) corresponding to the heavy precipitation associated with a severe thunderstorm along the Virginia–North Carolina border on 29 June 1986. (a) Radar-measured reflectivities. (b) Reflectivities deduced from the retrieval scheme applied to the aircraft measured brightness temperatures.

case). A second source of discrepancy may be the inability of even the 18-GHz radiances to fully penetrate storms containing very heavy precipitation. In extreme rainfall cases such as this, it may not be possible to retrieve near surface rainfall with greater accuracy than the 40% obtained here unless lower microwave frequencies are available.

4. Conclusions

This study presents the first quantitative retrieval of vertical profiles of hydrometeor density derived from multispectral microwave radiometry. Because data were available from five channels, the profiles are limited to a characterization of no more than five values that could be derived from the retrieval. This creates a very "blocky" result for the displayed image. Any refinement of these results requires either a substantial increase in the number of radiometric channels or the availability of spaceborne radar data, such as proposed for TRMM. Because the retrieved structures are constrained by the set of cloud structures available to the retrieval, some care should be exercised in selecting both the total number and the nature of these structures. While it is desirable to construct many diverse cloud models in order to cover all possible structures, an excessively large set of cloud models can easily become a computational burden. Thus, although com-

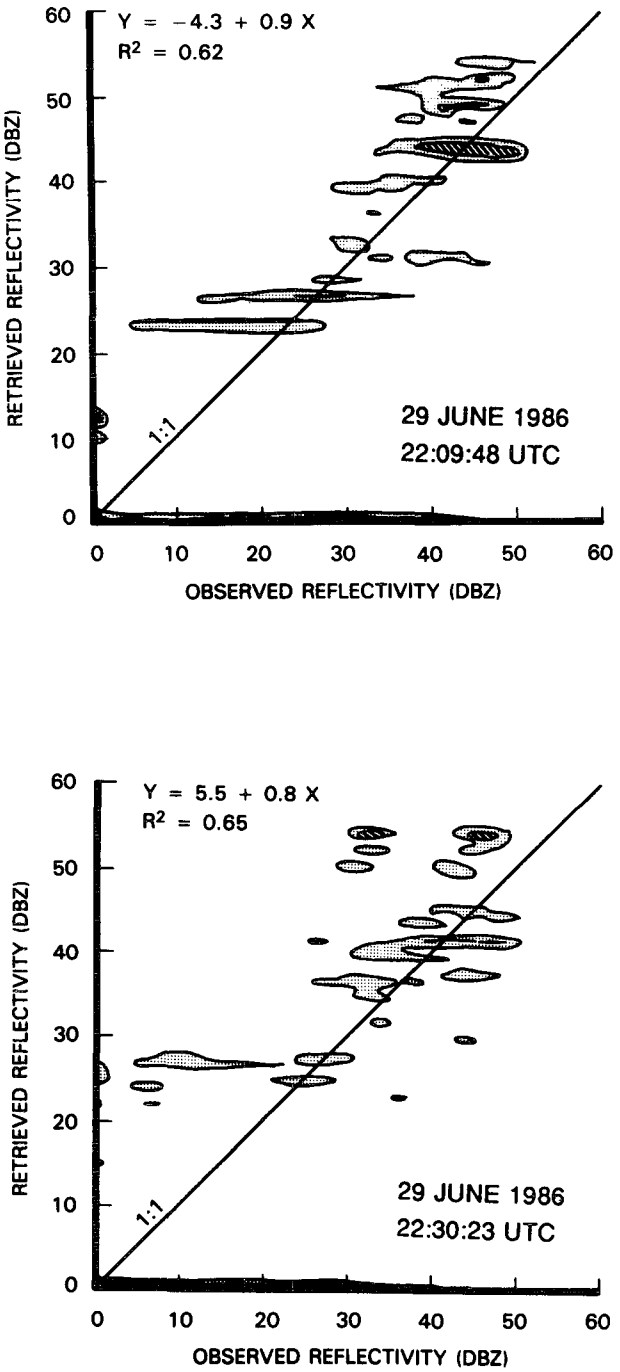

FIG. 6. Scatter plots showing correlation between radar reflectivities and retrieved reflectivities for the 29 June 1986 case study. Shaded contours represent regions containing more than 200 and 500 points with the same observed and retrieved reflectivities.

putational efficiency was not a factor in these case studies, the number of models was limited to relatively few (25) in order to illustrate that even a limited set of models can adequately capture the vertical structure of the precipitation. The present technique works best over ocean surfaces, where precipitating clouds present sufficient contrast against the background. The situation over land is more restrictive, because the contrast is adequate only for frequencies > 30 GHz. The problem is further complicated if the footprints become so large that only small portions of them are filled by rain.

For global applications of the above algorithm, it is necessary to automate the procedure. This task may be accomplished by simply testing all candidate cloud models and then selecting the particular structure that produces the least overall mean square difference between observed and retrieved brightness temperatures. For global datasets, it is further important to construct cloud structures that are suitable to various climatic regimes. To retrieve extratropical winter precipitation, for instance, it may be necessary to construct cloud structures whose freezing level is considerably lower than the 4-km freezing level used in this study.

While the radiometrically retrieved precipitation profiles have less vertical resolution than those that can be obtained from radar, such profiles can provide constraints on hydrometeor profiles that may be measured from a radar viewing the same part of the atmosphere. Employing radars and radiometers on board the same platform should thus yield a synergism that takes advantage of the complementary information from both sensors (Weinman et al. 1988). The present results were obtained from airborne radiometers, however the technique is applicable, in principle, to spaceborne measurements.

Cloud dynamical models (Tao et al. 1989) may be used to gain insight into the relationship between vertical hydrometeor structure and latent heating profiles. Information regarding the global distributions of latent heating in the atmosphere may serve to enhance the understanding and prediction of climatic variations such as El Niño or the North American drought of 1988.

Acknowledgments. The authors thank Dr. Robert Adler for his continuing support of the aircraft microwave studies. We would also like to thank Mr. Lafayette Long for help in preparing the final figures. This research was supported by the NASA Mesoscale Atmospheric Processes Research Program under the direction of Dr. James Dodge.

REFERENCES

Adler, R. F., H.-Y. M. Yeh, N. Prasad, J. Simpson, R. A. Mack and I. M. Hakkarinen, 1990: Aircraft microwave observations and simulations of deep convection at 18–183 GHz. Part I: Observations. *J. Atmos. Oceanic Tech.*, **7**, 392–410.

Chang, A. T. C., and A. S. Milman, 1982: Retrieval of ocean and atmospheric parameters from multichannel microwave radiometric measurements. *IEEE Trans. on Geosci. Remote Sens.*, **20**, 217–224.

Dodge, J., J. Arnold, G. Wilson, J. Evans and T. Fujita, 1986: The Cooperative Huntsville Meteorological Experiment. *Bull. Amer. Meteor. Soc.*, **67**, 417–419.

Houze, R. A., Jr., 1982: Cloud clusters and large-scale vertical motions in the tropics. *J. Meteor. Soc. Japan,* **60,** 396–410.

Kummerow, C., 1987: Microwave radiances from horizontally finite, vertically structured clouds. Ph.D. thesis, Univ. of Minnesota, Minneapolis, MN, 146 pp. [Available from University Microfilms, Ann Arbor, Michigan.]

——, and J. A. Weinman, 1988: Radiative properties of deformed hydrometeors at commonly used passive microwave frequencies. *IEEE Trans. Geosci. Remote Sens.,* **26,** 629–639.

——, R. A. Mack and I. M. Hakkarinen, 1989: A self-consistency approach to improve microwave rainfall rate estimation from space. *J. Appl. Meteor.,* **28,** 869–884.

Lau, K. M., and L. Peng, 1987: Origin of low-frequency (intraseasonal) oscillations in the tropical atmosphere. Part I: The basic theory. *J. Atmos. Sci.,* **44,** 950–972.

Marshall, J. S., and W. M. Palmer, 1948: The distribution of raindrops with size. *J. Meteor.,* **5,** 165–166.

Pichugin, A. P. and Yu G. Spiridonov, 1987: The spatial structure of precipitation zones on space-acquired imagery. Sov. J. Remote Sensing, **5,** 203–216. [English Translation]

Ramana Murty, Bh. V., A. K. Roy and K. R. Biswas, 1965: Radar echo intensity below the bright band. *J. Atmos. Sci.,* **22,** 91–94.

Simpson, J., R. F. Adler and G. North, 1988: A proposed tropical rainfall measuring mission (TRMM) satellite. *Bull. Amer. Meteor. Soc.,* **69,** 278–295.

Smith, E. A., and A. Mugnai, 1989: Radiative transfer to space through a precipitating cloud at multiple microwave frequencies. Part III: Influence of large ice particles. *J. Meteor. Soc. Japan,* **67.**

Smith, P. L., 1984: Equivalent radar reflectivity factors for snow and ice particles. *J. Climate Appl. Meteor.,* **23,** 1258–1260.

Tao, W.-K., J. Simpson, S. Lang, M. McCumber, R. Adler and R. Penc, 1990: An algorithm to estimate the heatingh budget from hydrometeor distributions. *J. Appl. Meteor.,* **29,** 1232–1244.

Theon, J. S., and N. Fugono, 1988: *Tropical Rainfall Measurement.* A. Deepak Publishing, 528 pp.

Trenberth, K. E., G. W. Branstator and P. A. Arkin, 1988: Origins of the 1988 North American drought. *Science,* **242,** 1640–1645.

Vivenkanandan, J., J. Turk, G. L. Stephens and V. N. Bringi, 1989: Microwave radiative transfer studies using combined multiparameter radar and radiometer measurements during COHMEX. *J. Appl. Meteor.,* **29,** 561–585.

Weinman, J. A., C. Kummerow and C. A. Atwater, 1988: An algorithm to derive precipitation from a downward viewing radar and a multifrequency passive radiometer. *Proc. IGARSS 88,* Edinburgh, U.K., 229–233.